Global and Planetary Change 148 (2017) 105–112

Contents lists available at ScienceDirect

Global and Planetary Change

journal homepage: www.elsevier.com/locate/gloplacha

ENSO response to external forcing in CMIP5 simulations of the last millennium

Thanh Le

Department of Geology, Quaternary Sciences, Lund University, 223 62 Lund, Sweden

ARTICLE INFO

Article history:
Received 28 February 2015
Received in revised form 29 August 2015
Accepted 9 December 2016
Available online 11 December 2016

Keywords:
Solar forcing
Volcanic forcing
Greenhouse gases radiative forcing
Granger causality
Last millennium
ENSO

ABSTRACT

The El Niño–Southern Oscillation (ENSO) is dominant mode of interannual climate variability, but its response to external climate forcings remains uncertain. Past studies have limitations including the use of short datasets and the uncertainty contained in reconstructions or simulations of past ENSO variations. To improve our understanding on ENSO variations, it is important to examine its response to these forcings by using multi model simulations since they provide longer datasets and help improving the statistical significance of the results. In this study, Granger causality test is applied to investigate the influence of external forcings on ENSO by using past millennium simulations (period 850–1850 CE) of Coupled Model Intercomparison Project Phase 5 (CMIP5) models. The results show robust influence of volcanic forcing to ENSO during preindustrial times of last millennium. The response of ENSO to solar forcing is more likely to be weak. Detection of GHGs variations signal in ENSO response is not significant. However, this study also indicates that there are uncertainties in the responses of ENSO to solar forcing and GHGs radiative forcing. The possibility of the true causal connection between Total Solar Irradiance (TSI) or GHGs radiative forcing and ENSO cannot be rejected at 95% significance level.

1. Introduction

The El Niño–Southern Oscillation (ENSO) is dominant mode of interannual climate variability and understanding its response to external forcings (i.e. solar forcing, volcanic radiative forcing and greenhouse gases radiative forcing) is of great interest.

The link between ENSO and solar forcing has remained unclear and it is difficult to detect (Cobb et al., 2003, 2013). While D'Arrigo et al. (2005) conclude that period of high variance ENSO index coincides with low radiative forcing period, Emile-Geay et al. (2007) suggest that large or moderate scenario of solar forcing have influence on ENSO variability at century-to-millennial-scale. Several studies emphasize the importance of ocean-atmosphere coupling mechanisms in the influence of solar forcing on tropical Pacific (Misios and Schmidt, 2012) and the importance of Bjerknes feedback in the connection between solar forcing or volcanic forcing and ENSO strength in the past 1000 years (Cane, 2005).

Recent studies showed a doubling in the occurrences of extreme El Niño events (Cai et al., 2014) and a near doubling in the frequency of future extreme La Niña events (Cai et al., 2015) in response to simulated future greenhouse warming. Besides, the influence of future increased greenhouse gases (GHGs) concentrations on the frequency of central Pacific El Niño and eastern Pacific El Niño is suggested for several models best able to simulate observations (Yeh et al., 2009; Power et al., 2013). However, such changes in ENSO characteristics are normally not consistent between all model simulations (Power et al., 2013).

The connection between explosive volcanic eruptions and ENSO has remained controversial. Several studies of both proxy data and model simulations suggested an association between volcanic eruptions and ENSO events (Handler, 1984; Adams et al., 2003; Mann et al., 2005; McGregor et al., 2010; McGregor and Timmermann, 2011; Wahl et al., 2014; Maher et al., 2015). In contrast, other studies found that the influences of volcanic radiative forcing (VRF) on ENSO are weak (Robock et al., 1995; Self et al., 1997; Ding et al., 2014). Previous studies might only use a small number of volcanic eruptions and there is uncertainty contained in reconstructions or simulations of past ENSO variations. These limitations might affect the statistical significance for establishing the true linkage between volcanic eruptions and ENSO. Moreover, past studies only investigate the VRF-ENSO relationship without accounting for the effects of other confounding factors (i.e. solar forcing, GHGs radiative forcing). These factors might have impacts on the ENSO and thus omitting these factors can lead to false conclusion about true VRF-ENSO relationship.

The current observational records are not long enough to investigate the response of ENSO to external forcings. Detecting the signal of external forcing in the variations of ENSO is difficult because of the large intrinsic changes in ENSO behavior (Collins et al., 2010). However, this problem can be solved by using large multi-model results, which consider that internal variability is taken into account.

E-mail address: Thanh.Le@geol.lu.se.

http://dx.doi.org/10.1016/j.gloplacha.2016.12.002
0921-8181/

Here, the author evaluates the causal relationship between external forcings and ENSO of past 1000-yr model simulations using multivariate vector autoregressive time series models and Granger causality tests (See Methods Section 2). This method accounts for the simultaneous effects of different factors (i.e. solar forcing, VRF and GHGs radiative forcing), thus, it might show a more clearly picture of ENSO response to external forcings. The current study is independent from previous studies in both aspects of datasets and statistical methods used. The results of this study might also serve as a test for the consistency of climate models in simulating the response of ENSO to external forcings.

2. Data

Monthly mean near-surface air temperature (TAS) data is used from the Coupled Model Intercomparison Project Phase 5 (CMIP5) model simulations of past 1000-yr (Taylor et al., 2012). The data is available for the period from 850 to 1850 CE. Thus, in this study, the last millennium refers to this period. The models were forced with Total Solar Irradiance reconstructions from either Delaygue and Bard (2010) or Vieira et al. (2011) or Steinhilber et al. (2009) or Wang et al. (2005), as shown in Table 1. Table 1 also shows the volcanic forcing (from either Crowley et al. (2008) or Gao et al. (2008)) used in each simulation (See Fig. 1 for the time series of these climate forcings). Other forcings include well-mixed greenhouse gases (GHGs) variations, orbital variations, land cover change and solar-related ozone change. The full details of climate forcing reconstruction options used in CMIP5 past 1000-yr simulations are described in Schmidt et al. (2011) and Schmidt et al. (2012).

The simulation of ENSO in CMIP5 models is an important aspect and it is discussed in previous studies. The large diversity in ENSO amplitude between models is improved in CMIP5 models compared to CMIP3 models (Bellenger et al., 2014). Though 50% of CMIP5 models cannot simulate the strength of EP and CP ENSOs, the spatial pattern and inter-model difference are improved (Kim and Yu, 2012). The observed intensity and the location of maximum SST anomalies are well captured in CMIP5 models of historical simulation. However, there are biases associated with the westward extent of SST anomalies (Taschetto et al., 2014). Besides, CMIP5 models still have systematical narrow bias in the simulated ENSO meridional width of SST anomaly (Zhang and Jin, 2012). Although CMIP5 models still have biases in simulating ENSO variability, these models provide valuable datasets to understand the response of ENSO to external forcings.

3. Methods

The ENSO index is defined as the leading empirical orthogonal function (EOF) of the winter (December–January–February) sea surface temperature (SST) anomalies in the Niño3.4 region (120°W-170°W; 5°N-5°S). The leading EOF reflects El Niño or La Niña pattern, featuring warm or cool anomalies of central Pacific SST in Niño3.4 region. This EOF mode explains 65–90% of total variance, depending on specific model. The changes of ENSO of past 1000-year is highly model dependent (See Fig. 2 for filtered ENSO time series of individual models). However, the range of simulated ENSO's amplitude is consistent between models, except the wide spread of ENSO's amplitude in the model MIROC-ESM (solid green line).

Note that the results of the relationship between ENSO and external forcings show no significant change if Niño3 (region of 90°W-150°W; 5°N-5°S) and Niño4 (region of 150°W-160°E; 5°N-5°S) indices are used. The analysis based on tropical Pacific region (100°E-70°W; 30°N-30°S) also has similar results (See Section 4.3 for brief discussion).

Multivariate vector autoregressive (VAR) time series models (e.g. Mosedale and Stephenson, 2006; Stern and Kaufmann, 2013) is used to estimate the influence of external forcings (i.e. solar forcing, volcanic forcing and GHGs radiative forcing) to ENSO. This method uses the definition of Granger causality (Granger, 1969) as follows: A variable Y has causal impact on another variable X if the knowledge of the past values of Y is useful in improving the prediction of X. The p^{th} order vector autoregressive VAR(p) is defined by:

$$X_t = \sum_{i=1}^{p} \alpha_i X_{t-i} + \sum_{i=1}^{p} \beta_i Y_{t-i} + \sum_{j=1}^{m} \sum_{i=1}^{p} \delta_{j,i} Z_{j,t-i} + \varepsilon_t \tag{1}$$

where X_t is the ENSO index at year t, Y_t is the considered forcing at year t, $Z_{j,t}$ is the control forcing j at year t, m is total number of control forcings, and $p \geq 1$ is the order of the causal model. The considered forcing is either Total Solar Irradiance (TSI) or volcanic radiative forcing (VRF) or GHGs radiative forcing. The forcing other than considered forcing is control forcing (or control variable (Stern and Kaufmann, 2013) or confounding factor (Hegerl et al., 2010)). Control forcings might have effects on the relationship between considered forcing and ENSO. In Eq. (1), m equals to 2, indicating that there are two control forcings. The terms α_i, β_i and $\delta_{j,i}$ are regression coefficients, ε_t is noise residual in the regression. The data of X, Y and $Z_{1 \to m}$ are detrended and normalized to produce stationary time series before computation.

Granger causality test (e.g. Mosedale and Stephenson, 2006; Le, 2014) is applied for the causal model shown in Eq. (1). This test accounts for the optimal order p for the VAR time series models by using Schwarz criterion or Bayesian information criterion (Schwarz, 1978). This criterion is required to avoid the model to become overly complex (i.e. too many parameters are added to the model). The optimal order is normally <8 for our current datasets. Thus, in our analysis, the maximum order is set at 8, indicating that the influence of external forcing to ENSO is only investigated at lagged timescale shorter than 10-year. The model given in Eq. (1) is complete model. The null model of no causality from Y to X is obtained by setting the $\{\beta_i; i = 1, 2, \ldots, p\}$ coefficients to zero. These two models are compared using the log likelihood ratio statistic:

$$L_{Y \to X} = n\left(\log\left|\Omega_{p,\beta_i=0}\right| - \log\left|\Omega_p\right|\right) \tag{2}$$

where $|\Omega_p|$ is the determinant of the covariance matrix of the residual, n is the sample size.

If the statistic $L_{Y \to X}$ in Eq. (2) is close to zero, then the null model is as equally good as the complete model in predicting the data of X, thus, Y has no causal impact on X. If this statistic is large, then the additional terms of Y help to predict the variability of X and we say that there is Granger causality. Statistical significance of the test is evaluated by comparing the $L_{Y \to X}$ statistic against the χ_p^2null distribution. If the p-value is smaller than 0.05, then the null hypothesis of no Granger causality is rejected at 5% level of significance.

Table 1
Last Millennium modelling institutes and model IDs and volcanic and solar forcing[a].

Institute	Model ID	Abbreviation	Volcanic forcing	Solar forcing
BCC	BCC-CSM1-1	BCC	GRA	VSK and WLS
NASA-GISS	GISS-E2-R	NASA	CEA	SBF
IPSL	IPSL-CM5A-LR	IPSL	GRA	VSK and WLS
LASG - IAP	FGOALS-s2	LASG-IAP	GRA	VSK and WLS
MIROC	MIROC-ESM	MIROC	CEA	DB and WLS
MPI-M	MPI-ESM-P	MPI-M	CEA	VSK and WLS
MRI	MRI-CGCM3	MRI	GRA	DB and WLS
NCAR	CCSM4	NCAR	GRA	VSK
UOED	HadCM3	UOED	CEA	SBF and WLS
UNSW	CSIRO-Mk3L-1-2	UNSW	CEA	SBF

[a] CEA = Crowley et al. (2008), DB = Delaygue and Bard (2010), GRA = Gao et al. (2008), SBF = Steinhilber et al. (2009), VSK = Vieira et al. (2011), WLS = Wang et al. (2005). The forcings of model GISS-E2-R are shown for selected ensemble of r1i1p121.

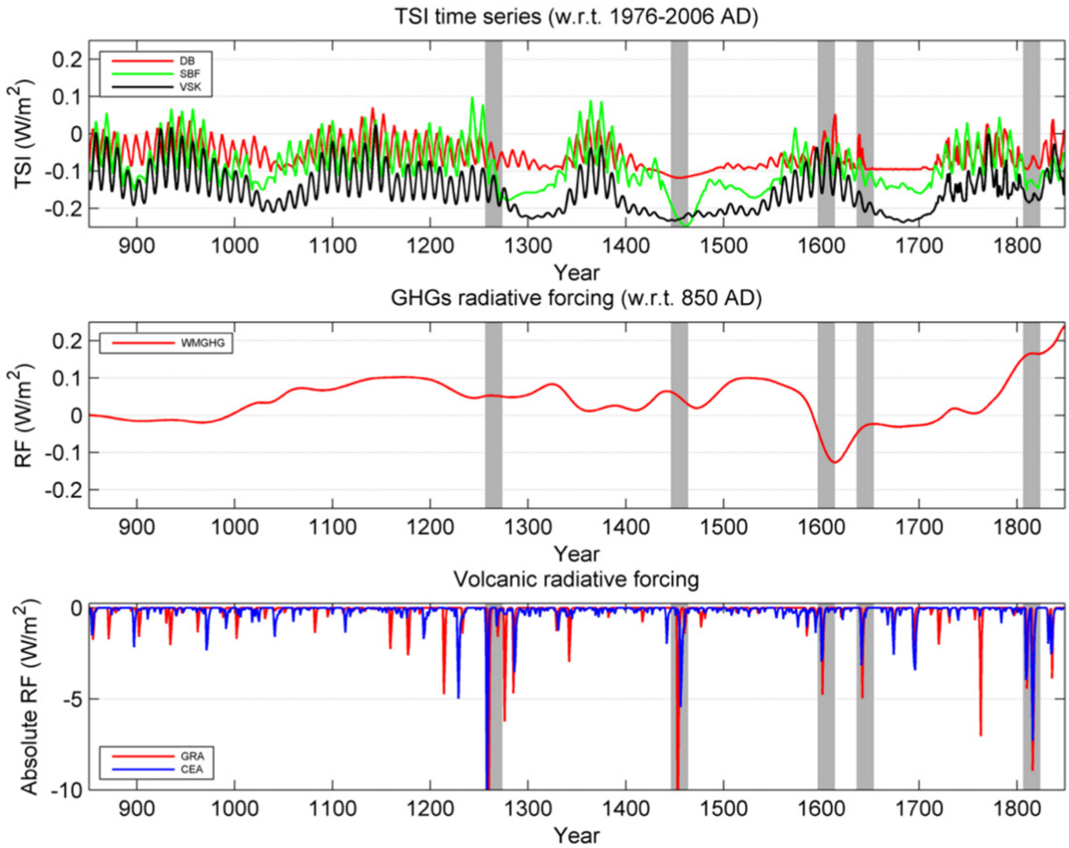

Fig. 1. Solar forcing, GHGs radiative forcing and volcanic forcing for period 850–1850 CE, respectively (see Table 1 for details of climate forcing reconstruction options used in CMIP5 past 1000-yr simulations). Solar forcing (from DB, VSK and SBF) is shown as TSI with respect to (w. r. t.) mean TSI of the period 1976–2006. GHGs radiative forcing is shown w. r. t. radiative forcing (RF) of the year 850. Volcanic RF is shown as absolute RF. Grey bars denote periods of large volcanic eruptions that coincide with periods of low ENSO index (See Fig. 2).

Monte Carlo simulation method is used to generate pseudo data of X, Y and $Z_{1\rightarrow m}$ and repeat the Granger causality test described above to estimate the p-value of no Granger causality. Ten thousands (10000) trials were performed to assure the convergence of the p-value. It is estimated that the relative error of that p-value is smaller than 1% if more trials were completed (e.g. increasing the trials to 50,000 provides identical results and the relative error is <1%).

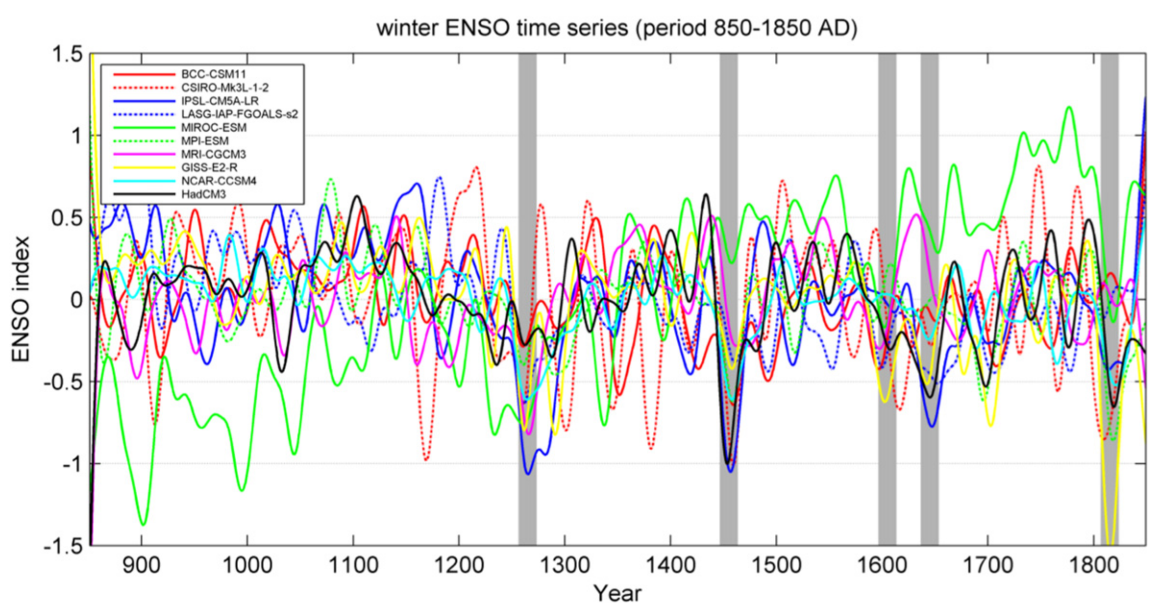

Fig. 2. ENSO index is defined as the leading empirical orthogonal function of the winter (December–January–February) sea surface temperature anomalies in the Niño3.4 region (120°W-170°W; 5°N-5°S). The ENSO index is shown for individual model. The time series are shown as 15-yr low-pass-filtered data. Grey bars denote periods of low ENSO index that coincide with periods of large volcanic eruptions (see also Fig. 1).

4. Results and discussions

4.1. Solar forcing and ENSO

Fig. 3 shows the probability of no Granger causality between solar forcing and ENSO of individual models. The result demonstrates that solar activity is not detected to have significant causal influence on ENSO variations. In Fig. 3, all models fail to reject the null hypothesis of no Granger causality between TSI and ENSO at 5% (or even 10%) significance level. There are 6 out of 10 models showing the *p*-values higher than 50%, indicating that a weak ENSO response to TSI in short term is more preferred between models. This result might suggest that solar forcing cannot trigger, statistically, ENSO events. The changes of ENSO require changes in background climate state of the tropical Pacific Ocean which is described by the intensity of the trade winds and spatially averaged depth of the thermocline (Fedorov and Philander, 2000). The result suggests that solar forcing might not produce different background states for the changes of ENSO. The result presented here shows an agreement with previous study (Cobb et al., 2003) based on paleo-ENSO reconstruction which suggests that ENSO variations of the last millennium are driven from the dynamics of the ENSO system itself rather than being influenced by solar forcing. Besides, ENSO variability is shown to have no systematic trend in the past 7000 years and the forced change in ENSO is difficult to detect (Cobb et al., 2013). Although several studies (Meehl et al., 2008; Le, 2014) show that solar forcing might alter tropical Pacific surface temperature, the weak response of ENSO to solar forcing suggests the likelihood that internal variability and other forcings, rather than solar forcing, dominate the predictability of ENSO statistics.

However, in Fig. 3, the probability of no Granger causality does not pass 95% significance level for most models (except MRI-CGCM3). Thus, one cannot reject the possibility of the true causal connection between TSI and ENSO at high significance level (e.g. 95% significance level). Hence, the linkage between TSI and ENSO in short term of <10-year remains partly unclear. In fact, several studies suggest the influence of solar forcing on tropical Pacific and ENSO strength at decadal time scales (Cane, 2005; Misios and Schmidt, 2012) rather than shorter time scales. This connection is also suggested to be significant at century-to-millennial time scales for large or moderate scenario of solar forcing and the ENSO might be a mediator between solar forcing and the Earth's climate (Emile-Geay et al., 2007). To provide more clearly evidence on this linkage, analysis of additional model simulations of longer period is necessary.

4.2. GHGs variations and ENSO

Detection of GHGs variations signal in ENSO response is not significant, suggesting that this forcing is not the main driver of ENSO variations of the last millennium (Fig. 4). In Fig. 4, most models (except BCC-CSM1-1) show the probability of no Granger causality between GHGs radiative forcing and ENSO higher than 50%. This result supports the possibility of weak sensitivity of the ENSO to GHGs variations. Figs.s 1 & 2 show that the decrease in GHGs radiative forcing in early seventeenth century occurs simultaneously with the reduction of ENSO index. Nevertheless, this reduction of ENSO index might be attributed to increased volcanic activity in this period rather than the decrease in GHGs radiative forcing. The weak connection of ENSO and GHGs variations found here is consistent between models. However, the possibility of a causal relationship between ENSO and GHGs variations cannot be ruled out at significance level higher than 90% for most models. This suggests that there are still uncertainties in this linkage. There are few studies that suggest the influence of GHGs variation in surface temperature response since late seventeenth century (Hegerl et al., 2011) and during 1600–1800 (Schurer et al., 2013). However, the signal of GHGs variations in ENSO response is not detected in past 1000 years. Other studies reported diverging responses of ENSO

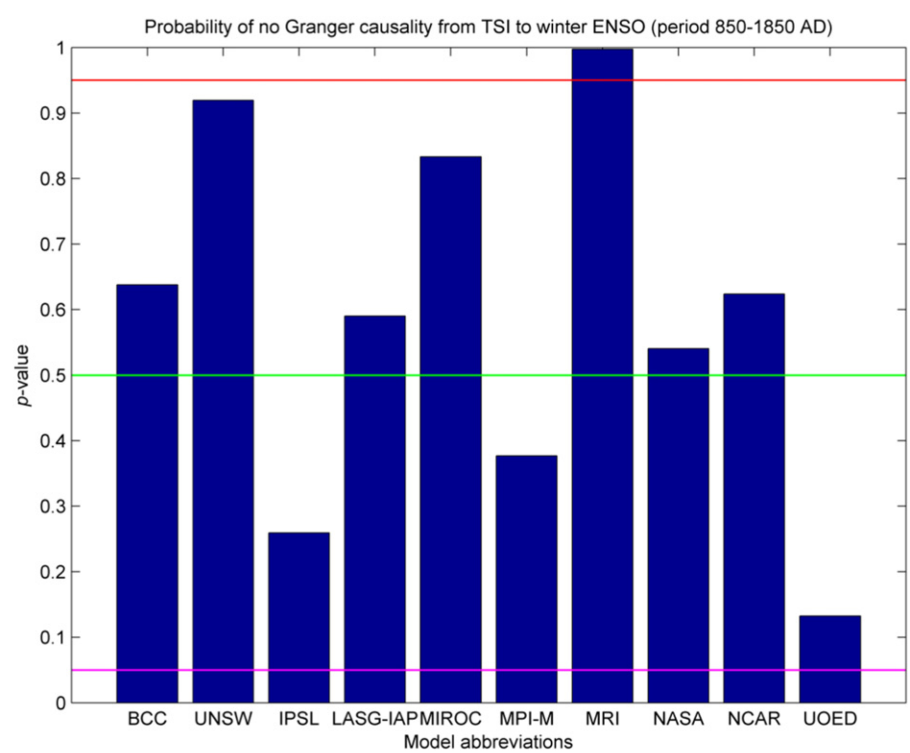

Fig. 3. Probability of no Granger causality from TSI to ENSO. Probability (*p*-value) is shown for individual model (See also Table 1 for model abbreviations). Horizontal red (green and magenta) line marks *p*-value of 0.95 (0.5 and 0.05). Models with *p*-value higher than 0.05 fail to reject the null hypothesis of no Granger causality between TSI and ENSO at 5% significance level.

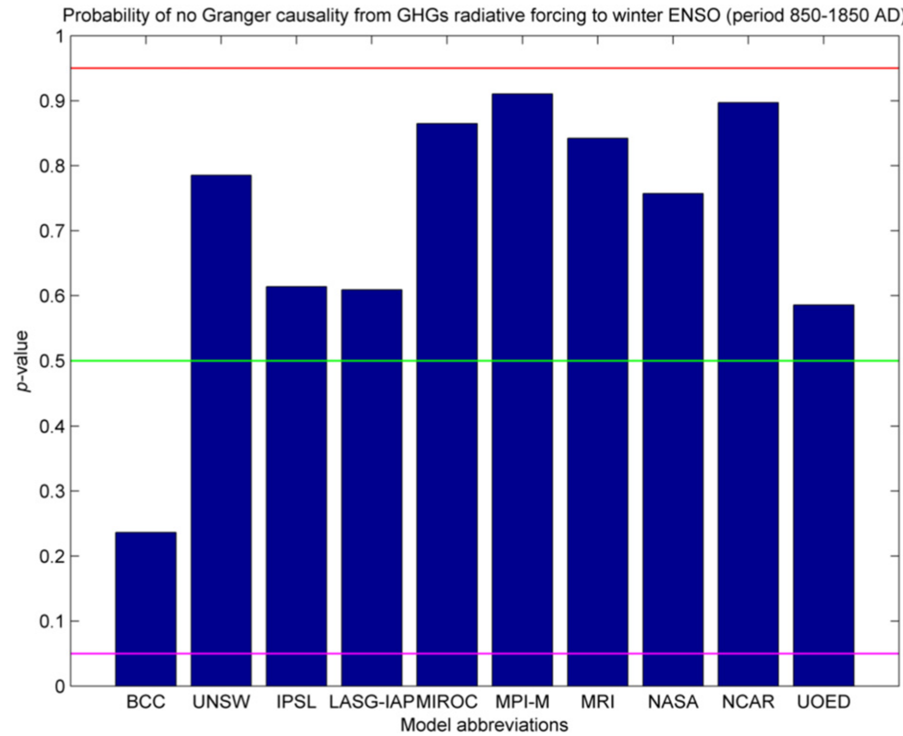

Fig. 4. As in Fig. 3 but for Granger causality from well-mixed greenhouse gases radiative forcing to ENSO.

to GHGs variations and these responses are attributed to different mechanisms (Philip and van Oldenborgh, 2006; DiNezio et al., 2012). The changes in ENSO amplitude under CO_2 doubling are related to variations of ocean heat flux convergence. The responses of mean climate to CO2 doubling include the weakening of the Walker circulation and the increased thermal stratification. While the first process reduces the ENSO amplitude, the second one increases the ENSO amplitude (DiNezio et al., 2012). Regarding the response of ENSO to increased CO_2 only, several studies focus on the change in ENSO amplitude with simulations in which the CO_2 concentration increases by 1% per year compound to twice of the pre-industrial value over given period. The results of these studies show inconsistency between models. For example, the amplitudes of ENSO under CO_2 doubling might increase or decrease depending on model simulations (Merryfield, 2006). Besides, there is only one out of six models selected show the sensitivity of ENSO amplitudes to CO_2 doubling (Yeh et al., 2006).

4.3. Volcanic forcing and ENSO

ENSO variations during preindustrial times of the last millennium appear to be dominated by volcanic forcing rather than solar forcing or GHGs radiative forcing (Fig. 5). Significant causal impact of VRF to ENSO at 5% significance level is found in 6 out of 10 models. This result indicates that most ENSO events during the last 1000-yr might be predictable few years in advance by using VRF. Volcanic eruptions influence the climate system by injecting aerosols into the atmosphere, and the distribution of volcanic aerosols is located in fairly uniform zonal band. Hence, VRF and the p-value are dependent on latitudinal bands. Here, the p-value shown in Fig. 5 is obtained by computing the mean of all p-values at different latitudinal bands. It should be noted that there is insensitive feedback of ENSO to VRF at high latitudes (i.e. 30–90 N band) in several models (i.e. MIROC-ESM, MPI-ESM-P, and HADCM3), although, the response of ENSO to VRF at other latitudes (i.e. 30–90 S, 0–30 S and 0–30 N bands) is significant in these models (see Supporting Fig. S1 for the response of ENSO to VRF at different latitudes). Other models show consistent influence of VRF to ENSO for all latitudes. If the bias of ENSO response to high latitudes VRF is neglected, there would be 8 out of 10 models (except BCC-CSM1-1 and FGOALS-s2) showing significant impact of VRF on ENSO. Given the fact that model simulations have used a number of different forcing histories of solar forcing and volcanic forcing (See Table 1), it suggests that the uncertainties and the biases associated with the response of ENSO to external forcings are minimized. Thus, this consistent result between models supports a clear evidence of systematic signature of VRF in ENSO response during past 1000-yr.

The mechanisms associated with the connection of VRF and ENSO have been suggested in previous studies. Volcanic eruptions can induce fast tropical and subtropical cooling (Mignot et al., 2011) and surface circulation at global scale (Handler, 1989), thus, it might trigger ENSO events. Besides, the influence of volcanic forcing on ENSO can be amplified by the Bjerknes feedback (Bjerknes, 1969; Cane, 1986) with cooling condition in the eastern tropical Pacific associated with reduced VRF (Cane, 2005). The response of ENSO to volcanic forcing can also be explained by the ocean dynamical thermostat mechanism (Clement et al., 1996) which is related to the creation of zonal temperature gradient in the tropical Pacific. Furthermore, the response of tropical Pacific Ocean to volcanic forcing might be related to four different variables, including the mean upwelling of anomalous temperatures, the zonal equatorial gradients of the mean cloud albedo, Newtonian cooling, and mixed layer depth (McGregor and Timmermann, 2011). Close inspection of the time series of the ENSO and VRF during past 1000-yr reveals that increased volcanism results in immediate decrease in ENSO index (See Figs. 1 and 2). These characteristics can be seen in the thirteenth, fifteenth, seventeenth and eighteenth centuries which are associated with large volcanic eruptions. Besides, the decreased solar forcing in mid fifteenth and early eighteenth centuries might enhance the rapid downtrend of ENSO during these periods. This result shows an agreement with previous study which suggests robust influence of large volcanic eruptions on ENSO variability over the past seven centuries (Li et al., 2013). ENSO is suggested as an event-like which requires an external initiating impulse to break the stable basic state in the tropical Pacific (Kessler, 2002). The results of this study demonstrate that VRF might be that initiating impulse and the likelihood of volcanic eruptions followed by ENSO events in short period of <10 years is significant. In

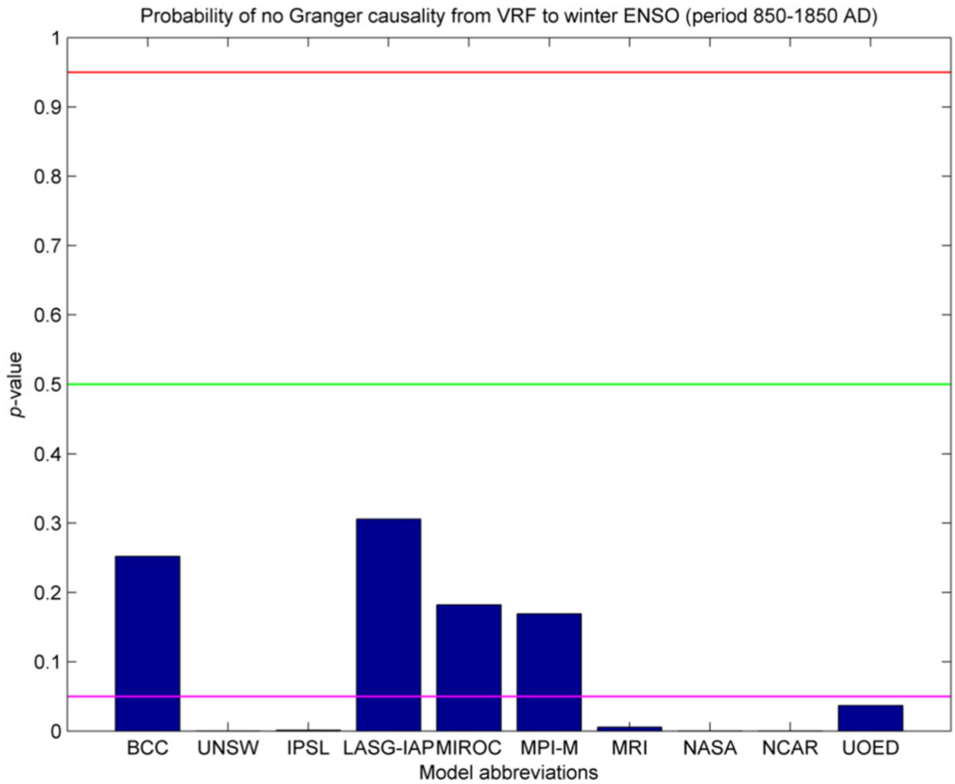

Fig. 5. As in Fig. 3 but for Granger causality from volcanic radiative forcing (VRF) to ENSO. There are six models showing Granger causality between VRF and ENSO at 5% significance level. See also Supporting Fig. S1 for the response of ENSO to VRF at different latitudes.

fact, past studies using proxy data have shown that robust La Niña-like response occurs in years 3–5 after eruption (Wahl et al., 2014) and composite responses of both El Niño and La Niña are found in years 0–7 after eruption (Adams et al., 2003). However, these studies only use volcanic events extending back to 1500. The result presented here shows that VRF significantly affects ENSO for a long period of 1000-yr rather than only short period of large volcanic eruptions. This conclusion is in contrast with previous studies (Robock et al., 1995; Self et al., 1997; Emile-Geay et al., 2008; Ding et al., 2014) which suggest small or no influence of volcanic eruptions to ENSO.

It is noted that the relationship between ENSO and external forcings show no significant change if Niño3 and Niño4 indices are used, instead of Niño3.4 index (See Figs. S2 & S3 for the response of Niño3 and Niño4 indices to external forcings). The analysis based on tropical Pacific region is shown in Fig. S4. However, we also note that Niño4 index, featuring SST anomalies in western tropical Pacific, is slightly more sensitive to VRF than Niño3.4 index, featuring SST anomalies in central tropical Pacific. Fig. S2a shows the sensitivity of Niño3 index to solar forcing with 7 out of 10 models having the p-values lower than 50% (model HadCM3 has the p-value lower than 5%). This result indicates that eastern tropical Pacific SST might be more sensitive to short term solar variations compared to western and central tropical Pacific SST.

5. Summary and conclusions

In this study, Granger causality test is applied to examine the influence of external forcings to El Niño–Southern Oscillation (ENSO) using past millennium simulations of Coupled Model Intercomparison Project Phase 5 (CMIP5) models. To my knowledge, this is the first time that ten different models have been used in a causal analysis that considers the short-term impacts of external forcings to ENSO.

The results indicate that ENSO variability of the past 1000 years is more likely to reflect weak sensitivity to solar forcing and GHGs radiative forcing, though, low solar forcing might enhance the rapid downtrend of ENSO during several periods. The probability of no Granger causality between TSI (or GHGs radiative forcing) and ENSO is higher than 50% for most models (See Figs. 3 & 4). Thus, a weak ENSO response to TSI (or GHGs radiative forcing) in short term is more preferred between models. The results of this study strengthen the conclusion of the insensitivity of ENSO to GHGs variations which has been shown in several studies (e.g. Knutson et al., 1997; Yeh et al., 2006). However, one cannot reject the possibility of the true causal connection between TSI (or GHGs radiative forcing) and ENSO at high significance level (e.g. 95% significance level). Hence, it is concluded that the linkage between TSI (or GHGs radiative forcing) and ENSO in short term of $<$10-year remains unclear.

Although the variations of ENSO is caused simultaneously by the chaotic behavior of tropical Pacific SST and by external radiative forcings (Vecchi and Wittenberg, 2010) and much of ENSO variations of the last 1000-yr might be caused by internal variability of the coupled ocean–atmosphere system (Knutson et al., 1997), this study with large ensemble of model simulations reveals a significant response of ENSO to VRF. These findings, though based on model simulations, are statistically significant. The robust causal influence of VRF to ENSO shows an agreement with past studies (Adams et al., 2003; McGregor et al., 2010; Li et al., 2013; Wahl et al., 2014) which suggest the evidence of this linkage in proxy data. This implies that the capability of several CMIP5 models is sufficient to reproduce the signal of volcanic forcing in ENSO response. The results of this study underline the importance of VRF in Earth's climate system of the last 1000-year. The role of VRF in the climate system might be much more significant than that of other forcings.

The possibility of long-term impacts of solar forcing to ENSO and the uncertainties that might be contained in the response of ENSO to solar forcing or GHGs variations underscore the necessity for more understanding of the dynamical response of ENSO to external forcings. The results presented here need to be further examined with additional model simulations of longer period, especially regarding the linkages between solar forcing or GHGs variations and ENSO.

Acknowledgement

The author thanks Jesper Sjolte for helpful discussions. I acknowledge the World Climate Research Programme's Working Group on Coupled Modelling, which is responsible for CMIP, and I thank the climate modelling groups (listed in Table1 of this paper) for producing and making available their model output. For CMIP the U.S. Department of Energy's Program for Climate Model Diagnosis and Intercomparison provides coordinating support and led development of software infrastructure in partnership with the Global Organisation for Earth System Science Portals. The author thanks the anonymous reviewer and the Editor for their insightful comments. The research work reported herein was sponsored by a grant from the strategic research program of ModElling the Regional and Global Earth system (MERGE), hosted by the Faculty of Science at Lund University. I thank the Fysiografiska Sällskapet i Lund (Physiographic Society in Lund) for financial support.

Appendix A. Supplementary data

Supplementary data to this article can be found online at http://dx.doi.org/10.1016/j.gloplacha.2016.12.002.

References

Adams, J., Mann, M., Ammann, C., 2003. Proxy evidence for an El Nino-like response to volcanic forcing. Nature 426:274–278. http://dx.doi.org/10.1038/nature02087.1 (November).

Bellenger, H., Guilyardi, E., Leloup, J., Lengaigne, M., Vialard, J., 2014. ENSO representation in climate models: from CMIP3 to CMIP5. Clim. Dyn. 42 (7–8):1999–2018. http://dx.doi.org/10.1007/s00382-013-1783-z.

Bjerknes, J., 1969. Atmospheric Teleconnections from the equatorial Pacific. Mon. Weather Rev. 97 (3):163–172. http://dx.doi.org/10.1175/1520-0493(1969)097<0163:ATFTEP>2.3.CO;2.

Cai, W., et al., 2014. Increasing frequency of extreme El Niño events due to greenhouse warming. Nat. Clim. Chang. 5 (2):1–6. http://dx.doi.org/10.1038/nclimate2100.

Cai, W., et al., 2015. Increased frequency of extreme La Niña events under greenhouse warming. Nat. Clim. Chang. 5 (2):132–137. http://dx.doi.org/10.1038/nclimate2492.

Cane, M.A., 1986. El Niño. Annu. Rev. Earth Planet. Sci. 14:43–70. http://dx.doi.org/10.1146/annurev.ea.14.050186.000355.

Cane, M.A., 2005. The evolution of El Niño, past and future. Earth Planet. Sci. Lett. 230 (3–4):227–240. http://dx.doi.org/10.1016/j.epsl.2004.12.003.

Clement, A.C., Seager, R., Cane, M.A., Zebiak, S.E., 1996. An ocean dynamical thermostat. J. Clim. 9 (9):2190–2196. http://dx.doi.org/10.1175/1520-0442(1996)009<2190:AODT>2.0.CO;2.

Cobb, K.M., Charles, C.D., Cheng, H., Edwards, R.L., 2003. El Nino/Southern Oscillation and tropical El Nino Pacific climate during the last millennium. Nature 424, 271–276 (July).

Cobb, K.M., Westphal, N., Sayani, H.R., Watson, J.T., Di Lorenzo, E., Cheng, H., Edwards, R.L., Charles, C.D., 2013. Highly variable El Niño-Southern Oscillation throughout the Holocene. Science 339 (6115):67–70. http://dx.doi.org/10.1126/science.1228246.

Collins, M., et al., 2010. The impact of global warming on the tropical Pacific Ocean and El Niño. Nat. Geosci. 3 (6):391–397. http://dx.doi.org/10.1038/ngeo868.

Crowley, T., Zielinski, G., Vinther, B., 2008. Volcanism and the Little Ice Age. :pp. 4–5 http://dx.doi.org/10.1029/2002GL0166335.

D'Arrigo, R., Cook, E.R., Wilson, R.J., Allan, R., Mann, M.E., 2005. On the variability of ENSO over the past six centuries. Geophys. Res. Lett. 32 (3):L03711. http://dx.doi.org/10.1029/2004GL022055.

Delaygue, G., Bard, E., 2010. An Antarctic view of beryllium-10 and solar activity for the past millennium. Clim. Dyn. 36 (11–12):2201–2218. http://dx.doi.org/10.1007/s00382-010-0795-1.

DiNezio, P.N., Kirtman, B.P., Clement, A.C., Lee, S.-K., Vecchi, G.a., Wittenberg, A., 2012. Mean climate controls on the simulated response of ENSO to increasing greenhouse gases. J. Clim. 25 (21):7399–7420. http://dx.doi.org/10.1175/JCLI-D-11-00494.1.

Ding, Y., Carton, J., Chepurin, G.A., Stenchikov, G., Robock, A., Sentman, L.T., Krasting, J.P., 2014. Ocean response to volcanic eruptions in coupled model intercomparison project 5 simulations. J. Geophys. Res.:5622–5637 http://dx.doi.org/10.1002/2013JC009780.Received.

Emile-Geay, J., Cane, M., Seager, R., Kaplan, A., Almasi, P., 2007. El Niño as a mediator of the solar influence on climate. Paleoceanography 22 (3). http://dx.doi.org/10.1029/2006PA001304.

Emile-Geay, J., Seager, R., Cane, M.a., Cook, E.R., Haug, G.H., 2008. Volcanoes and ENSO over the past millennium. J. Clim. 21 (13):3134–3148. http://dx.doi.org/10.1175/2007JCLI1884.1.

Fedorov, A.V., Philander, S.G., 2000. Is El Niño changing? Science 288 (44), 1997–2002 (80-).

Gao, C., Robock, A., Ammann, C., 2008. Volcanic forcing of climate over the past 1500 years: an improved ice core-based index for climate models. J. Geophys. Res. 113 (D23):D23111. http://dx.doi.org/10.1029/2008JD010239.

Granger, C., 1969. Investigating causal relations by econometric models and cross-spectral methods. J. Econ. Soc. 37 (5), 424–438.

Handler, P., 1984. Possible association of stratospheric aerosols and El Nino type events. Geophys. Res. Lett. 11 (11), 1121–1124.

Handler, P., 1989. The effect of volcanic aerosols on global climate. J. Volcanol. Geotherm. Res. 37 (3–4):233–249. http://dx.doi.org/10.1016/0377-0273(89)90081-4.

Hegerl, G., Luterbacher, J., González-Rouco, F., Tett, S.F.B., Crowley, T., Xoplaki, E., 2011. Influence of human and natural forcing on European seasonal temperatures. Nat. Geosci. 4 (2):99–103. http://dx.doi.org/10.1038/ngeo1057.

Hegerl, G.C., Hoegh-Guldberg, O., Casassa, G., Hoerling, M.P., Kovats, R.S., Parmesan, C., Pierce, D.W., Stott, P.A., 2010. Good practice guidance paper on detection and attribution related to anthropogenic climate change. In: Stocker, T.F., Field, C.B., Qin, D., Barros, V., Plattner, G.-K., Tignor, M., Midgley, P.M., Ebi, K.L. (Eds.), Meeting Report Of The Intergovernmental Panel On Climate Change Expert Meeting On Detection And Attribution Of Anthropogenic Climate Change. IPCC Working Group I Technical Support Unit, University of Bern, Bern, Switzerland.

Kessler, W.S., 2002. Is ENSO a cycle or a series of events? Geophys. Res. Lett. 29 (23):1–4. http://dx.doi.org/10.1029/2002GL015924.

Kim, S.T., Yu, J.Y., 2012. The two types of ENSO in CMIP5 models. Geophys. Res. Lett. 39 (11):1–6. http://dx.doi.org/10.1029/2012GL052006.

Knutson, T.R., Manabe, S., Gu, D., 1997. Simulated ENSO in a global coupled ocean-atmosphere model: Multidecadal amplitude modulation and CO2 sensitivity. J. Clim. 10 (1994):138–161. http://dx.doi.org/10.1175/1520-0442(1997)010<0138:SEIAGC>2.0.CO;2.

Le, T., 2014. Solar forcing of Earth's surface temperature in PMIP3 simulations of the last millennium. Atmos. Sci. Lett. http://dx.doi.org/10.1002/asl2.555.

Li, J., et al., 2013. El Niño modulations over the past seven centuries. Nat. Clim. Chang. 3 (9):822–826. http://dx.doi.org/10.1038/nclimate1936.

Maher, N., Mcgregor, S., England, M.H., Sen Gupta, A., 2015. Effects of volcanism on tropical variability. Geophys. Res. Lett. http://dx.doi.org/10.1002/2015GL064751.Over.

Mann, M., Cane, M., Zebiak, S.E., Clement, A., 2005. Volcanic and solar forcing of the tropical Pacific over the past 1000 years. J. Clim. 447–456.

McGregor, S., Timmermann, A., 2011. The effect of explosive tropical volcanism on ENSO. J. Clim. 24 (8):2178–2191. http://dx.doi.org/10.1175/2010JCLI3990.1.

McGregor, S., Timmermann, A., Timm, O., 2010. A unified proxy for ENSO and PDO variability since 1650. Clim. Past 6 (1):1–17. http://dx.doi.org/10.5194/cp-6-1-2010.

Meehl, G.A., Arblaster, J.M., Branstator, G., van Loon, H., 2008. A coupled air–sea response mechanism to solar forcing in the Pacific region. J. Clim. 21 (12):2883–2897. http://dx.doi.org/10.1175/2007JCLI1776.1.

Merryfield, W.J., 2006. Changes to ENSO under CO2 doubling in a multimodel ensemble. J. Clim. 19 (16):4009–4027. http://dx.doi.org/10.1175/JCLI3834.1.

Mignot, J., Khodri, M., Frankignoul, C., Servonnat, J., 2011. Volcanic impact on the Atlantic Ocean over the last millennium. Clim. Past 7 (4):1439–1455. http://dx.doi.org/10.5194/cp-7-1439-2011.

Misios, S., Schmidt, H., 2012. Mechanisms involved in the amplification of the 11-yr solar cycle signal in the tropical Pacific Ocean. J. Clim. 25 (14):5102–5118. http://dx.doi.org/10.1175/JCLI-D-11-00261.1.

Mosedale, T., Stephenson, D., 2006. Granger causality of coupled climate processes: ocean feedback on the North Atlantic Oscillation. J. Clim. 1182–1194.

Philip, S., van Oldenborgh, G.J., 2006. Shifts in ENSO coupling processes under global warming. Geophys. Res. Lett. 33 (11):L11704. http://dx.doi.org/10.1029/2006GL026196.

Power, S., Delage, F., Chung, C., Kociuba, G., Keay, K., 2013. Robust twenty-first-century projections of El Niño and related precipitation variability. Nature 502 (7472): 541–545. http://dx.doi.org/10.1038/nature12580.

Robock, A., Taylor, K., Georgiy, Stenchikov, L., Liu, Y., 1995. GCM evaluation of a mechanism for El Niño triggering by the El Chichón ash cloud. Geophys. Res. Lett. 22 (17), 2369–2372.

Schmidt, G.A., et al., 2011. Climate forcing reconstructions for use in PMIP simulations of the last millennium (v1.0). Geosci. Model Dev. 4 (1):33–45. http://dx.doi.org/10.5194/gmd-4-33-2011.

Schmidt, G.A., et al., 2012. Climate forcing reconstructions for use in PMIP simulations of the Last Millennium (v1.1). Geosci. Model Dev. 5 (1):185–191. http://dx.doi.org/10.5194/gmd-5-185-2012.

Schurer, A.P., Hegerl, G.C., Mann, M.E., Tett, S.F.B., Phipps, S.J., 2013. Separating forced from chaotic climate variability over the past millennium. J. Clim. 26 (18): 6954–6973. http://dx.doi.org/10.1175/JCLI-D-12-00826.1.

Schwarz, G., 1978. Estimating the dimension of a model. Ann. Stat.

Self, S., Rampino, M., Zhao, J., Katz, M.G., 1997. Volcanic aerosol perturbations and strong El Nino events: no general correlation. Geophys. Res. Lett. 24 (10), 1247–1250.

Steinhilber, F., Beer, J., Fröhlich, C., 2009. Total solar irradiance during the Holocene. Geophys. Res. Lett. 36 (19):L19704. http://dx.doi.org/10.1029/2009GL040142.

Stern, D.I., Kaufmann, R.K., 2013. Anthropogenic and natural causes of climate change. Clim. Chang. 122 (1–2):257–269. http://dx.doi.org/10.1007/s10584-013-1007-x.

Taschetto, A.S., Sen Gupta, A., Jourdain, N.C., Santoso, A., Ummenhofer, C.C., England, M.H., 2014. Cold tongue and warm pool ENSO events in CMIP5: mean state and future projections. J. Clim. 27 (8):2861–2885. http://dx.doi.org/10.1175/JCLI-D-13-00437.1.

Taylor, K.E., Stouffer, R.J., Meehl, G.A., 2012. An overview of CMIP5 and the experiment design. Bull. Am. Meteorol. Soc. 93 (4):485–498. http://dx.doi.org/10.1175/BAMS-D-11-00094.1.

Vecchi, G.a., Wittenberg, A.T., 2010. El Niño and our future climate: where do we stand? Wiley Interdiscip. Rev. Clim. Chang. 1. http://dx.doi.org/10.1002/wcc.33 ((April), n/a–n/a).

Vieira, L.E.A., Solanki, S.K., Krivova, N.A., Usoskin, I., 2011. Evolution of the solar irradiance during the Holocene. Astron. Astrophys. 531 (A6). http://dx.doi.org/10.1051/0004-6361/201015843.

Wahl, E.R., Diaz, H.F., Smerdon, J.E., Ammann, C.M., 2014. Late winter temperature response to large tropical volcanic eruptions in temperate western North America: relationship to ENSO phases. Glob. Planet. Chang. 122:238–250. http://dx.doi.org/10.1016/j.gloplacha.2014.08.005.
Wang, Y., Lean, J., Jr, N.S., 2005. Modeling the Sun's magnetic field and irradiance since 1713. Astrophys. J. 522–538.
Yeh, S., Kug, J., Dewitte, B., Kwon, M., Kirtman, B.P., Jin, F., 2009. El Niño in a changing climate. Nature 461 (7263):511–514. http://dx.doi.org/10.1038/nature08316.
Yeh, S.-W., Park, Y.-G., Kirtman, B.P., 2006. ENSO amplitude changes in climate change commitment to atmospheric CO2 doubling. Geophys. Res. Lett. 33 (13):L13711. http://dx.doi.org/10.1029/2005GL025653.
Zhang, W., Jin, F.F., 2012. Improvements in the CMIP5 simulations of ENSO-SSTA meridional width. Geophys. Res. Lett. 39 (23):1–5. http://dx.doi.org/10.1029/2012GL053588.